

# Enhanced Block-Oriented Behavioral Model for the Linearization of Nonlinear Power Amplifiers with Strong Memory Effects

Marouan Othmani<sup>1</sup>, Manel Chouchane<sup>1</sup>, and Nouredine Boulejfen<sup>2</sup>

<sup>1</sup>Faculty of Sciences of Tunis, University of Tunis El Manar, Tunis, Tunisia

<sup>2</sup>Military Research Center, Tunis, Tunisia

## Abstract

This paper proposes a new behavioral model for the linearization of radio frequency (RF) power amplifiers (PAs) exhibiting strong nonlinear memory effects. The proposed model enhances the augmented Hammerstein model through the inclusion of cross-terms, and as a result, improved accuracy and linearization performance are achieved. This technique benefits from the advantages of block-based models and adds more robustness against strong nonlinear memory effects in wideband applications. A proof-of-concept prototype using a commercial PA was built in order to test and evaluate the linearization performance of the proposed DPD. The performance assessment was carried out using 5G new radio (NR) signals with a bandwidth of 40 MHz and a PAPR of 8 dB. The proposed predistorter showed better linearization performance compared to the conventional and augmented Hammerstein-based predistorters.

## Keywords

*Behavioral model, digital predistortion, linearization, memory effects, power amplifier*

## 1. Introduction

New fifth-generation (5G) mobile communication systems feature modulated signals with a high peak-to-average power ratio (PAPR) [1] [2]. However, signals with high PAPRs are critical for the performance of the transmitter, in particular, the power amplifier (PA). In fact, to achieve maximum efficiency, PAs need to be driven close to their saturation region, where, considering their nonlinear input-output relation, there will be considerable levels of distortion [1]-[3]. On the other hand, backing off the PA from saturation reduces the power efficiency. Therefore, a trade-off between linearity and efficiency has always been crucial in the design of PAs. To overcome this trade-off, linearization techniques can be used to maximize power efficiency and reduce the distortion level. The main linearization techniques are feedback, feedforward, and digital predistortion (DPD) [3]-[9]. Indeed, DPD is considered the dominant method for the linearization of PAs. DPD consists of applying digital signal processing techniques in order to compensate for the nonlinear distortions generated by the PA. To realize that, the inverse nonlinearity of the PA needs to be identified then included before the nonlinear device. As a result, the cascade of the

inverse nonlinearity and the PA would behave as a linear system.

In order to predict the behavior of the PA, various modeling techniques have been introduced in the literature [3]. One of the most used behavioral modeling methods is the memory polynomial model (MPM) as it allows compensating for the nonlinear distortions produced by PAs with memory effects. It has been proven that using the MPM results in high modeling and linearization performance. However, the implementation of this model adds hardware complexity caused by the large number of coefficients. For this reason, block-oriented modeling techniques that aim to reduce the computational complexity and improve the numerical stability are becoming more and more popular. Indeed, the Hammerstein model is considered one of the most used block-oriented models that tend to reduce the required number of coefficients, and therefore enhance the dispersion of coefficients and matrix conditioning. The Hammerstein behavioral model is based on combining a nonlinear memoryless function, such as a look-up table (LUT) model [3], [10]-[11], and a linear filter to predict the memory effects of the PA. This formulation showed reduced complexity in various systems in literature [3], [12]. However, the Hammerstein model only considers the linear memory effects of the PA, and considering the fact that new transmitter systems are required to support much higher bandwidths, both linear and nonlinear memory effects should be taken into account in the modeling process. In this context, the augmented Hammerstein model [3], [12]-[13] solves this issue by including nonlinear memory effects in the formulation of the model. Nevertheless, if the PA exhibits strong memory effects, the aforementioned formulations would provide a limited performance for wideband applications.

In this paper, we propose a new version of the augmented Hammerstein model that is able to predict the nonlinear behavior of PAs exhibiting strong nonlinear memory effects. The proposed technique enhances the augmented Hammerstein model through the inclusion of cross-terms, and therefore, improved linearization accuracy is achieved. The inclusion of cross-terms in the non-block-based models such as the generalized MPM (GMPM) and hybrid MPM (HMPM) has shown significant

improvement in the modeling and linearization performances [14], [15]. However, this principle has never been applied in the block-based modeling context. This technique maintains the low complexity provided by the block-oriented models, and at the same time offers more robustness against strong memory effects in wideband applications.

This paper is organized as follows. In section II, we describe the DPD principle and provide an overview of the behavioral modeling techniques used in the literature to predict the behavior of RF PAs. In section III, we present the proposed model. Section IV describes the measurement setup and the evaluation procedure used in this work. The experimental results are given in section V. Finally, we provide the conclusion in section VI.

## 2. Behavioral Modeling and Digital Predistortion of RF Power Amplifiers

### 2.1 Digital Predistortion Principle

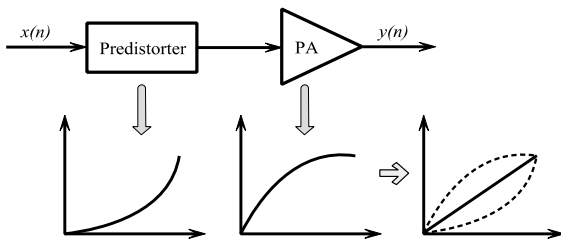


Fig. 1. Principle of the DPD linearization technique.

The principle of the DPD is illustrated in Fig. 1. It consists of pre-distorting the input signal in order to compensate for the distortions later generated by the PA. The result would be an undistorted signal at the output of the nonlinear device. The success of this technique came from the technological advances of digital signal processors (DSPs), analog-to-digital converters (ADCs), digital-to-analog converters (DAC), etc. In fact, since the DPD system is implemented in the digital domain, the configuration and parameters of the predistorter can be modified without changing the hardware structure of the transmission system.

### 2.2 Behavioral Modeling of Power Amplifiers

Various formulations have been introduced in the literature for the behavioral modeling and DPD of RF PAs. These can be classified according to several criteria, such as the number of boxes, inclusion or exclusion of memory effects, etc. In this section, we present the LUT, MPM, Hammerstein, and augmented Hammerstein models.

#### 2.2.1 Look-Up Table Model

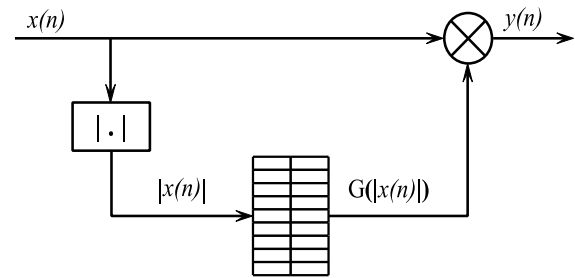


Fig. 2. Principle of the LUT model.

The LUT model shown in Fig. 2 is the basic behavioral modeling technique for memoryless PA nonlinearity. The magnitude of the input signal and the corresponding complex gain of the PA are stored in a LUT. The output waveform of the model is given by the following expression [10]-[12]

$$y(n) = G(|x|).x(n) \quad (1)$$

where  $x(n)$  and  $y(n)$  are the input and output complex waveforms of the model, respectively;  $G(|x|)$  is the complex gain of the LUT. Although most systems exhibit memory effects, LUT models are still employed to estimate the static nonlinearity box-based models, such as Hammerstein-based behavioral models and DPDs.

#### 2.2.2 Memory Polynomial Model

The MPM technique is widely used for the modeling and DPD of nonlinear PAs exhibiting memory effects. It corresponds to a simplification of the well-known Volterra series, where only the diagonal terms are kept. The MPM is expressed as follows

$$y(n) = \sum_{m=0}^M \sum_{k=1}^K a_{mk} \cdot x(n-m) \cdot |x(n-m)|^{k-1} \quad (2)$$

where  $y(n)$  and  $x(n)$  are the input and output waveforms of the model, respectively;  $a_{mk}$  are the model complex coefficients;  $K$  is the nonlinearity order;  $M$  is the memory depth.

The popularity of the MPM comes from its high performance in terms of modeling and linearization. However, the relatively large number of coefficients required for accurate modeling adds more hardware complexity to the system. This issue is more severe for high nonlinearity orders and memory depths.

### 2.2.3 Hammerstein Model

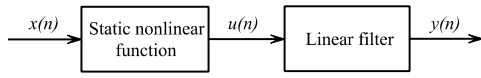


Fig. 3. Block diagram of the Hammerstein-based model.

The Hammerstein model is based on implementing a nonlinear memoryless function followed by a linear finite impulse response (FIR) filter [12],[13]. The principle of this technique is illustrated in Fig. 3. A LUT model can be used to perform the nonlinear memoryless function, and therefore the mathematical expressions of the Hammerstein model can take the following form

$$u(n) = G(|x(n)|).x(n) \quad (3)$$

and

$$y(n) = \sum_{m=0}^M a_m \cdot u(n - m) \quad (4)$$

where  $x(n)$  and  $y(n)$  are respectively the input signal and the estimated output of the system;  $u(n)$  is the output of the first block;  $G(|x|)$  is the complex instantaneous gain of the LUT;  $a_m$  and  $M$  are the complex coefficients and the memory depth of the FIR filter, respectively. The fact that the Hammerstein model uses linear filters to predict the memory effects of the PA limits the accuracy, as nonlinear memory effects are not considered.

### 2.2.4 Augmented Hammerstein Model

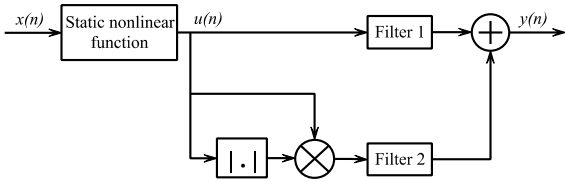


Fig. 4. Block diagram of the augmented Hammerstein-based model.

The augmented Hammerstein model [13] is considered as an extended version of the conventional formulation that includes the nonlinear memory effects component into the model, as shown in Fig. 4. If a LUT model is used for the static nonlinear function, the mathematical expressions of this system would be as follows

$$u(n) = G(|x(n)|).x(n) \quad (5)$$

and

$$y(n) = \sum_{m_1=0}^{M_1} a_{m_1} \cdot u(n - m_1) + \sum_{m_2=0}^{M_2} b_{m_2} \cdot u(n - m_2) \cdot |u(n - m_2)| \quad (6)$$

where  $x(n)$  and  $y(n)$  are the input and estimated output of the system, respectively;  $u(n)$  and  $G(|x|)$  are respectively the output and the complex gain of the static nonlinear function;  $M_1$  and  $M_2$  are the memory depth of the first and second filters, respectively;  $a_{m_1}$  and  $b_{m_2}$  are the filters' responses.

### 3. Proposed Box-Oriented Model

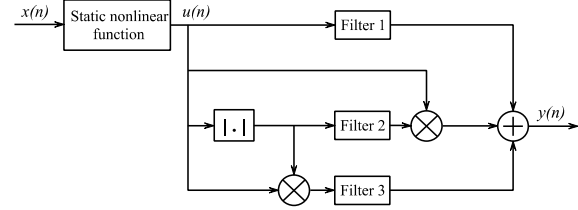


Fig. 5. Block diagram of the proposed model.

The proposed model aims to add more robustness to the system against strong nonlinear memory effects. It consists of including the cross-terms made of the actual sample of the signal and its lagging envelope samples.

Fig. 5 shows the principle of the proposed modeling technique. An additional FIR filter is applied to the envelope samples, and its output is multiplied by the complex sample of the signal. Then, the output is added to the outputs of the other filters. If a LUT is employed as the memoryless nonlinear function, we can express the proposed model by the following equations

$$u(n) = G(|x(n)|).x(n) \quad (7)$$

and

$$y(n) = \sum_{m_1=0}^{M_1} a_{m_1} \cdot u(n - m_1) + u(n) \cdot \sum_{m_2=0}^{M_2} b_{m_2} \cdot |u(n - m_2)| + \sum_{m_3=0}^{M_3} c_{m_3} \cdot u(n - m_3) \cdot |u(n - m_3)| \quad (8)$$

and therefore

$$y(n) = \sum_{m_1=0}^{M_1} a_{m_1} \cdot u(n - m_1) + \sum_{m_2=0}^{M_2} b_{m_2} \cdot u(n) \cdot |u(n - m_2)| + \sum_{m_3=0}^{M_3} c_{m_3} \cdot u(n - m_3) \cdot |u(n - m_3)| \quad (9)$$

where  $x(n)$  and  $y(n)$  are respectively the input and output of the model;  $u(n)$  and  $G(|x|)$  are the output and the complex instantaneous gain of the static nonlinear function, respectively;  $M_1$ ,  $M_2$ , and  $M_3$  are the memory depths of the linear filters;  $a_{m_1}$ ,  $b_{m_2}$ , and  $c_{m_3}$  are the filters' coefficients.

#### 4. Measurement Setup

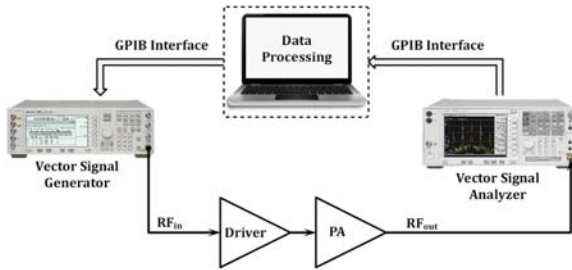


Fig. 6. Measurement setup used in this work.

Fig. 6 presents the evaluation setup of the model identification and PA linearization procedure. The main components are a data processing unit, a vector signal generator (VSG), a power amplification unit with relatively strong nonlinear memory effects, an attenuator, and a vector signal analyzer (VSA). The waveforms are generated in MATLAB then sent to the VSG for modulation and up-conversion. The power amplification unit boosts the power of the RF signal. Then, the amplified signal is attenuated and sent to the VSA for down-conversion and digitization. After that, gain normalization and time alignment between the received and generated data are performed in the computer. Finally, the data will be used for model identification and DPD. The tests were performed on 5G NR waveforms with a bandwidth of 40 MHz and a PAPR of 8 dB.

The linearization principle used for the evaluation of the proposed technique is illustrated in Fig. 7. The analog-to-digital and digital-to-analog converters (DAC and ADC, respectively) were designed in MATLAB. Both converters are based on delta-sigma modulators (DSMs). In fact, DSMs are known for their high performance in terms of resolution and noise shaping capability.

In this evaluation, three DPD systems were designed using the proposed-, Hammerstein-, and augmented Hammerstein-based configurations. The orders of the FIR filters were set to 3 and the static nonlinear functions were performed using LUT systems.

#### 5. Experimental Results

In this section, we present the obtained results of the proposed DPD in comparison with the conventional and augmented Hammerstein-based DPDs.

In order to evaluate the linearization performance, we have selected the adjacent channel power ratio (ACPR) and alternate channel power ratio (AltCPR) figures of merit to measure the spectral regrowth of the evaluated transmitters. The ACPR and AltCPR metrics quantify the average powers of the adjacent and alternate channels compared to the average power of the main channel. These metrics are expressed as follows

$$\text{ACPR(dBc)} = 10 \log_{10} \left( \frac{P_{adj}}{P_{main}} \right) \quad (10)$$

and

$$\text{AltCPR(dBc)} = 10 \log_{10} \left( \frac{P_{alt}}{P_{main}} \right) \quad (11)$$

where  $P_{adj}$  and  $P_{alt}$  are the average powers in the adjacent and alternate channels, respectively, and  $P_{main}$  is the average power of the main channel.

Fig. 8 shows the spectra of the proposed DPD compared to the ones based on the conventional and augmented Hammerstein models. In addition, the error spectra are shown in Fig. 9. It can be observed from the graphs in both figures that the proposed model outperformed the conventional formulations. In fact, it is clear from Fig. 8 that the introduced system was able to reduce the spectral regrowth the most compared to the other configurations. Moreover, from Fig. 9, we can see that the lowest error was provided by the proposed formulation. This is explained by the inclusion of the cross-terms component in the expression, and the consideration of both linear and nonlinear memory effects. For PAs with stronger nonlinear memory effects, the outperformance would be even greater, which confirms the effectiveness of using the introduced enhanced version of the model.

Table 1 summarizes the ACPRs and AltCPRs obtained by the evaluated DPDs.

Table 1: Summary of the ACPR and AltCPR values obtained using the proposed DPD in comparison with the conventional and augmented Hammerstein-based DPDs.

Architecture	ACPR (dBc)	
	Lower/Upper	AltCPR (dBc) Lower/Upper
Without DPD	-29.15/29.09	-45.24/-45.34
Hammerstein-based DPD	-44.96/-45.74	-51.33/-51.86
Augmented Hammerstein-based DPD	-50.10/-51.13	-55.15/-56.84
Proposed DPD	-53.55/-54.52	-57.02/-58.71

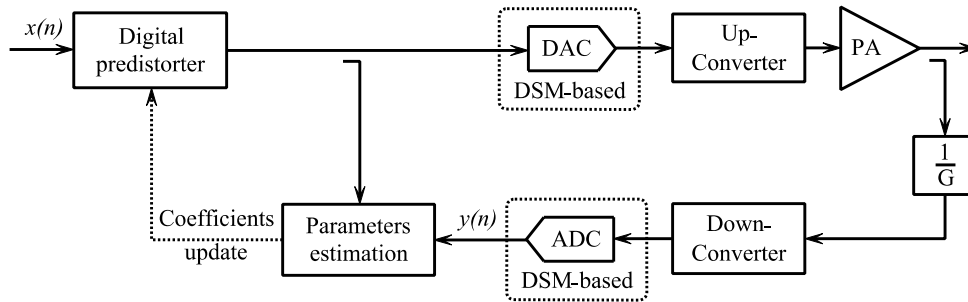


Fig. 7. Principle of the transmitter architecture used for the evaluation of the proposed DPD.

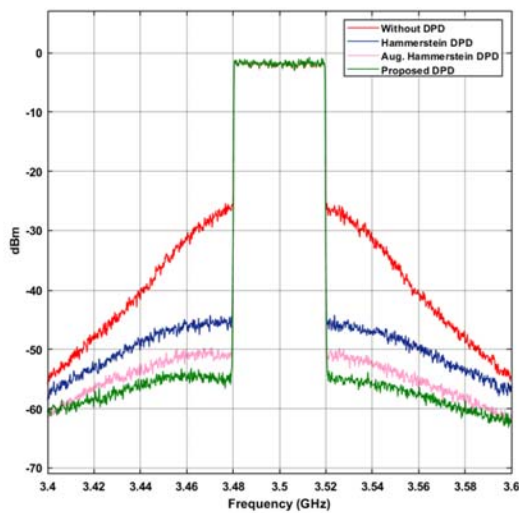


Fig. 8. Measured spectra obtained using the proposed DPD in comparison with the conventional and augmented Hammerstein-based DPDs.

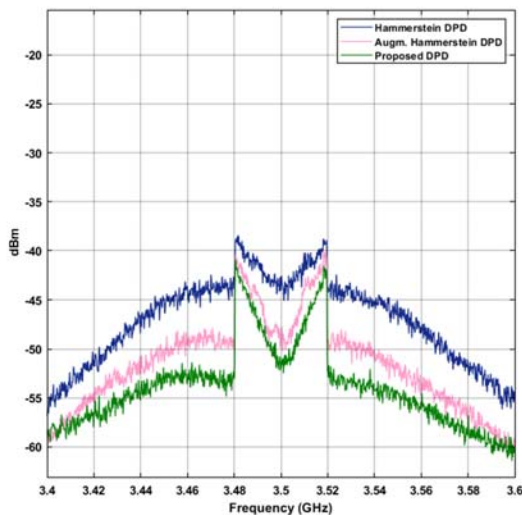


Fig. 9. Error spectra obtained using the proposed DPD in comparison with the conventional and augmented Hammerstein-based DPDs.

### 6. Conclusion

This paper proposed a new PA behavioral model for the linearization of nonlinear PAs exhibiting strong nonlinear memory effects. The proposed model enjoys the benefits of block-based models, and at the same time offers more robustness when wideband signals are used. This is achieved by the inclusion of the cross-terms component into the formulation of the augmented Hammerstein model. A comparison of the linearization performance was carried out using a commercial PA excited with a 5G NR signal with a bandwidth of 40 MHz and a PAPR of 8 dB. The higher performance is achieved by means of a larger number of parameters, but this increase is justified by the remarkable outperformance of the proposed technique in comparison with the conventional and augmented Hammerstein-based models.

### References

- [1] S. Cripps, *RF Power Amplifiers for Wireless Communications, Second Edition*, 2006.
- [2] B. Lathi and Z. Ding, *Modern Digital and Analog Communication Systems*, ser. Oxford Series in Electrical an. Oxford University Press, 2009.
- [3] F. M. Ghannouchi and O. Hammi, "Behavioral modeling and predistortion," *IEEE Microwave Magazine*, vol. 10, no. 7, pp. 52–64, 2009.
- [4] A. Katz, J. Wood, and D. Chokola, "The evolution of PA linearization: From classic feedforward and feedback through analog and digital predistortion," *IEEE Microwave Magazine*, vol. 17, no. 2, pp. 32–40, 2016.
- [5] J. Zhao, P. Liu, L. Zhai, and F. Yang, "A novel digital predistortion based on flexible characteristic detection for 5G massive MIMO transmitters," *IEEE Microwave and Wireless Components Letters*, pp. 1–4, 2021.
- [6] C. Yu, Q. Lu, H. Yin, J. Cai, J. Chen, X.-W. Zhu, and W. Hong, "Linear-decomposition digital predistortion of power amplifiers for 5G ultrabroadband applications," *IEEE Transactions on Microwave Theory and Techniques*, vol. 68, no. 7, pp. 2833–2844, 2020.

- [7] C. Yu, K. Tang, and Y. Liu, "Adaptive basis direct learning method for predistortion of RF power amplifier," *IEEE Microwave and Wireless Components Letters*, vol. 30, no. 1, pp. 98–101, 2020.
- [8] X. Wang, Y. Li, C. Yu, W. Hong, and A. Zhu, "Digital predistortion of 5G massive MIMO wireless transmitters based on indirect identification of power amplifier behavior with OTA tests," *IEEE Transactions on Microwave Theory and Techniques*, vol. 68, no. 1, pp. 316–328, 2020.
- [9] X. Wang, Y. Li, H. Yin, C. Yu, Z. Yu, W. Hong, and A. Zhu, "Digital predistortion of 5G multiuser MIMO transmitters using low-dimensional feature-based model generation," *IEEE Transactions on Microwave Theory and Techniques*, pp. 1–1, 2021.
- [10] S. Boumaiza, J. Li, M. Jaidane-Saidane, and F. Ghannouchi, "Adaptive digital/RF predistortion using a nonuniform LUT indexing function with built-in dependence on the amplifier nonlinearity," *IEEE Transactions on Microwave Theory and Techniques*, vol. 52, no. 12, pp. 2670–2677, 2004.
- [11] Q. A. Pham, D. Lopez-Bueno, T. Wang, G. Montoro, and P. L. Gilabert, "Partial least squares identification of multi look-up table digital predistorters for concurrent dual-band envelope tracking power amplifiers," *IEEE Transactions on Microwave Theory and Techniques*, vol. 66, no. 12, pp. 5143–5150, 2018.
- [12] T. Liu, S. Boumaiza, and F. Ghannouchi, "Deembedding static nonlinearities and accurately identifying and modeling memory effects in wide-band RF transmitters," *IEEE Transactions on Microwave Theory and Techniques*, vol. 53, no. 11, pp. 3578–3587, 2005.
- [13] —, "Augmented Hammerstein predistorter for linearization of broadband wireless transmitters," *IEEE Transactions on Microwave Theory and Techniques*, vol. 54, no. 4, pp. 1340–1349, 2006.
- [14] D. Morgan, Z. Ma, J. Kim, M. Zierdt, and J. Pastalan, "A generalized memory polynomial model for digital predistortion of RF power amplifiers," *IEEE Transactions on Signal Processing*, vol. 54, no. 10, pp. 3852–3860, 2006.
- [15] O. Hammi, M. Younes, and F. M. Ghannouchi, "Metrics and methods for benchmarking of PA transmitter behavioral models with application to the development of a hybrid memory polynomial model," *IEEE Transactions on Broadcasting*, vol. 56, no. 3, pp. 350–357, 2010.